Oriented Self-Assembly | Hot Paper

DOI: 10.1002/ange.201307897

Template-Assisted Self-Assembly: Alignment, Placement, and Arrangement of Two-Dimensional Mesostructured DNA–Silica Platelets**

*Ben Liu, Yuan Yao, and Shunai Che**

Highly ordered hierarchical biomolecule–inorganic structures, such as bone, dentine, eggshell, and marine mollusc shells, are ubiquitous in nature.[1] The artificial organization of nature-inspired, biomolecule-templated hierarchical inorganic materials is a key challenge in enabling many nanotechnological applications.[2] "Bottom-up" self-assembly is a widely applied strategy for synthesizing and fabricating ordered hierarchical/multilevel spatial structures or morphologies from components ranging from nanometers to micrometers in size. Alternatively, "top-down" lithographic approaches allow for arbitrary geometrical designs and superior nanometer-level precision, accuracy, and registration. Template-assisted self-assembly (TASA) combines bottom-up self-assembly with top-down patterned templates to eliminate defects and induce registration and orientation in thin-film materials, providing rich opportunities to produce biomimetic multilevel hierarchies.[3]

Using TASA, the orientation and periodicity of zero-dimensional (0D) spherical block copolymer microdomains, colloid crystals, and metal nanoparticles and 1D metal oxide nanotubes/nanowires were guided into 2D/3D hierarchical spatial architectures.[3a,d,4] In these systems, the use of biomolecular building blocks has attracted great attention because of their biocompatibility, inherent molecular-recognition properties, and facile use in bottom-up fabrication. Recently, DNA origami-like triangles (with precise banding of gold nanocrystals) were successfully placed and oriented on lithographically patterned surfaces.[5] These systems are the most typical examples of selectively aligning 2D assemblies to date. The successful selective alignment, placement, and arrangement of anisotropic 2D/3D hierarchically mesostructured assemblies with sufficient long-range order, however, have rarely been reported.[6]

[*] B. Liu, Dr. Y. Yao, Prof. Dr. S. Che
School of Chemistry and Chemical Engineering
State Key Laboratory of Metal Matrix Composites
Shanghai Jiao Tong University
800 Dongchuan Road, Shanghai, 200240 (P.R. China)
E-mail: chesa@sjtu.edu.cn
Homepage: http://che.sjtu.edu.cn

[**] We acknowledge the support of the 973 project (2009CB930403), the National Basic Research Program of China (2013CB934101), the National Natural Science Foundation (21101106) of China and Evonik Industries. We kindly thank Suzhou Institute of Nano-Tech and Nano-Bionics (SINTNO), Chinese Academy of Sciences (CAS) for preparing the lithographically patterned silicon substrates.

Supporting information for this article is available on the WWW under http://dx.doi.org/10.1002/anie.201307897.

DNA, which is one of the most attractive chiral biomolecules, has the ability to condense and self-assemble into multiple liquid-crystal phases, including blue phases, chiral cholesteric phases, and 2D columnar phases.[7] By employing a quaternary aminosilane (TMAPS, *N*-trimethoxysilylpropyl-*N*,*N*,*N*-trimethylammonium chloride) as both the condensing agent and the co-structure-directing agent (CSDA)[8] and tetraethyl orthosilicate (TEOS) as the inorganic source, we recently discovered a novel route for preparing 2D DNA–silica platelets (DSPs) with 2D square *p*4*mm* and 2D hexagonal *p*6*mm* symmetries through the self-assembly of DNA and silica mineralization.[9] The successful synthesis of DSPs provided a potential route for creating multilevel, hierarchically mesostructured spatial DNA–silica films (DSFs) by combining bottom-up self-assembly with a top-down lithographically patterned template (see the Supporting Information).

Our strategy was to selectively align, place, and arrange DSPs at different positions on patterned silicon substrate surfaces by thermodynamically and kinetically controlling DSP formation, which depends on the charge density of the quaternary ammonium groups, which in turn depends on their positions on the patterned silicon substrate, the ionization degree of DNA, and the TMAPS concentration. Herein, unpatterned silicon substrates were used to control the alignment of 2D DSPs, whereas silicon substrates that were lithographically patterned with 2D rectangles were used to selectively control the placement and arrangement of DSPs.

As the silanol-terminated surface was electrically neutral, the electrostatic interactions between DNA and the substrate surface were increased by the following procedure. The silicon substrates were sequentially cleaned with a solution of hydrofluoric acid (HF), acetone/ethanol, and deionized water three times. The surfaces were then chemically modified by silanization with TMAPS, which terminated the substrate surface (see the Supporting Information, Figure S1).[10] Then, the quaternary-ammonium-functionalized silicon substrates were immersed into a DSP synthesis gel to grow the DSFs in situ (see the Supporting Information). It should be noted that the glossy (unpatterned) and patterned sides of the silicon substrate were immersed face-down and horizontally into the upper part of the synthesis gel (Figure S2) to ensure that the DSPs grew on the substrate surface and were not deposited from the synthesis gel.

Scanning electron microscopy (SEM) and high-resolution transmission electron microscopy (HRTEM) images of the microscopic morphologies and mesostructures of DSFs that were grown on the unpatterned silicon substrates at different

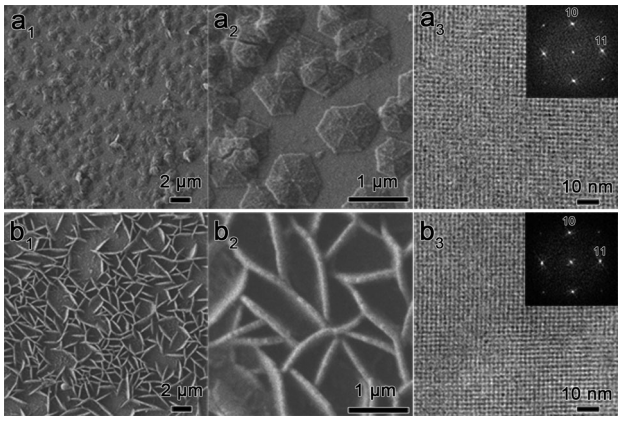

Figure 1. Alignment of 2D mesostructured DSPs on the surface of an unpatterned silicon substrate. Low- and high-magnification SEM images and corresponding HRTEM images of the DSFs at pH 4.6 (a_1–a_3) and 7.4 (b_1–b_3). The molar composition of the synthesis gel was DNA/TMAPS/TEOS/H_2O/HCl or NaOH = 1:6:15:18000:*x*, where *x* (HCl) = 0.3 (a) and *x* (NaOH) = 0.9 (b).

pH values of the synthesis gel are shown in Figure 1. At a lower pH values (< 4.9), the horizontally aligned 2D DSPs formed on the substrate surface were hexagonal and had diameters in the range of 0.8–1.2 μm (Figure 1 a_1, a_2).[9] In contrast, when the pH was increased to 5.4–8.8, randomly oriented hexagonal DSPs with diameters of 0.8–1.5 μm grew vertically on the substrate surface (Figure 1 b_1, b_2). The DSFs formed at intermediate pH (between 4.9 and 5.4) exhibited a mixture of horizontal and vertical alignment (Figure S3). HRTEM images showed that both the horizontally and vertically aligned DSPs had a highly ordered 2D square *p*4*mm* symmetry (Figure 1 a_3, b_3).[9,11] When the pH was increased to values above 9.2, the symmetry of DSP mesostructures that were vertically aligned on the substrate surface became 2D hexagonal *p*6*mm* (Figure S4).[11b] It can easily be imaged that the DNA molecules were vertically and horizontally arranged on the substrate surface in the horizontally and vertically aligned DSPs, respectively (Figure S1). Furthermore, the DSP diameter and density decreased with increasing TMAPS concentration (Figure S5).

The observed alignments of the DNA molecules and DSPs at different pH values can be explained in terms of the electrostatic interactions between DNA and the quaternary-ammonium-modified substrate. The ionization degree of the negatively charged phosphate groups on the DNA, which increases gradually with increasing pH,[12] is critical to the interactions between DNA and the positively charged silicon substrate. At a lower pH, the ionization degree of DNA was too low for DNA to interact with the quaternary ammonium groups on the substrate surface. In this case, the DNA molecules could not be electrostatically arranged on the surface, making it difficult to grow DSPs in situ. It is possible that the hexagonal DSPs might have formed in the synthesis gel and subsequently migrated and adhered to the substrate surface, where the DNA–silica complexes further condensed with TEOS, because of electrostatic interactions between the negatively charged silicate in the DSP framework and the positively charged quaternary ammonium groups on the surface. The preferential interaction between the surface and the larger sides of the hexagonal DSPs led to horizontal alignment on the surfaces (Figure S1, lower pH). In contrast, at a higher pH, the highly ionized DNA molecules interacted with each other along their helical axis and lay horizontally on the positively charged substrate surface to form flat DNA layers.[13] The DNA molecules subsequently self-assembled and grew epitaxially with TMAPS and TEOS, producing vertically aligned DSPs in situ (Figure S1, higher pH).[6]

Multilevel, hierarchical spatial architectures with selectively placed and oriented 2D DSPs were fabricated on lithographically patterned silicon substrates using TASA. For this purpose, 2D rectangles that were 0.5–3 μm wide (both grooves and protuberances) and approximately 200 nm deep were printed on the silicon substrates using lithography (Figure S6). The SEM images of DSFs that were synthesized on the patterned substrates with features that were 2 μm wide and approximately 200 nm deep are shown in Figure 2. The

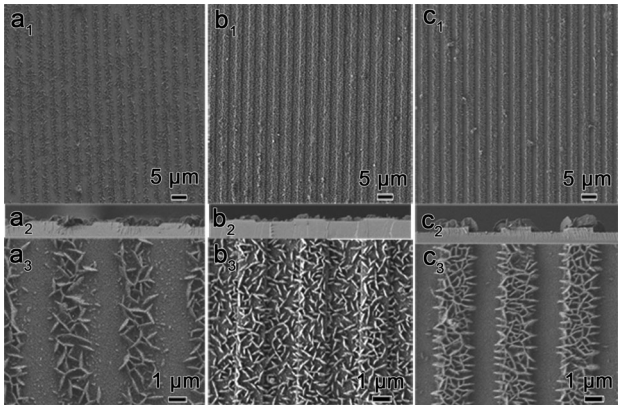

Figure 2. Placement of vertically aligned 2D mesostructured DSPs on the surface of a lithographically patterned silicon substrate. Top and side views of the low- and high-magnification SEM images of the DSFs synthesized with TMAPS concentrations of 7 mg mL^{-1} (a), 9 mg mL^{-1} (b), and 12 mg mL^{-1} (c). The pH of the reaction solution was ca. 5.8. The molar composition of the synthesis gel was DNA/TMAPS/TEOS/H_2O = 1:*x*:15:18000, where *x* = 3.5 (a), 4.5 (b), and 6 (c).

placement of the DSFs was controlled by changing the TMAPS concentration at lower pH values of the synthesis gel, but they exhibited an oriented arrangement only at higher pH and a higher TMAPS concentration. All DSPs were vertically aligned, which indicates that the DNA molecules were horizontally arranged on the substrate surfaces because of stronger electrostatic interactions between the negatively charged DNA and the positively charged quaternary ammonium groups on the substrate surface at higher pH values (compared pH 4.6, as shown in Figure 1 a). All of the DSPs assembled on the patterned substrate surfaces had 2D square *p*4*mm* mesostructures (Figure S7).

At a lower TMAPS concentration of approximately 7 mg mL^{-1}, a large proportion of vertically aligned 2D mesostructured DSPs with diameters of 0.8–1 μm were selectively placed in the grooves of the patterned substrate at a pH of approximately 5.8 (Figure 2 a_1–a_3). These small DSPs were similarly grown at a lower pH of 5.0 (Figure S8 a).

The selective placement of the vertically aligned 2D DSPs in the wider grooves also resulted in a similar assembly behavior and arrangement (Figure S9). When the TMAPS concentration was slightly increased to approximately 9 mg mL^{-1}, vertically aligned 2D DSPs grew indiscriminately (without selective placement) over the entire surface of the patterned substrate (Figure 2b and Figure S10). A further increase in the TMAPS concentration to approximately 12 mg mL^{-1} resulted in the selective placement of randomly oriented 2D mesostructured DSPs on the protuberances of the patterned substrates (Figure 2c$_1$–c$_3$).

Vertically aligned 2D mesostructured DSPs (similar to those shown in Figure 2c) were selectively placed on the protuberances with widths of 0.5–3 μm at a lower pH of approximately 5.8 and a higher TMAPS concentration of approximately 12 mg mL^{-1}, which indicates that this synthesis system is capable of selective placement (Figure 3). It should

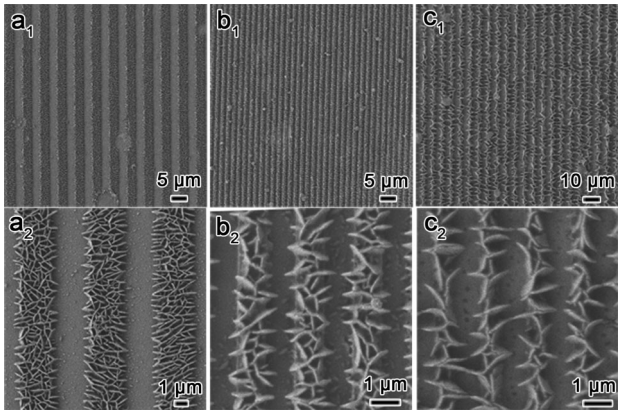

Figure 3. Placement of vertically aligned 2D mesostructured DSPs on the protuberances of silicon substrates with different patterned widths. Low- and high-magnification SEM images of DSFs synthesized on surfaces with patterned widths of 3 μm (a), 1 μm (b), and 0.5 μm (c). The pH of the reaction solution was approximately 5.8. The molar composition of the synthesis gel was DNA/TMAPS/TEOS/H_2O = 1:6:15:18000.

be noted that the DSPs at the groove edges were parallel to each other and perpendicular to the longitudinal direction of the rectangular pattern when the patterned width was as large as 2 μm (Figure 2c and Figure 3a). A similar long-range arrangement of randomly oriented DSPs in the grooves and parallel DSPs at the edges was clearly observed as the pH of the synthesis gel was gradually increased to 6.8 (Figure S8b).

When the pH was further increased to approximately 7.8, and a TMAPS concentration of 12 mg mL^{-1} was used, vertically aligned DSPs grew mostly at the edges and exhibited a long-range parallel alignment (perpendicular to the longitudinal direction of the pattern) regardless of the patterned width (1–3 μm; Figure 4). The DSP sizes in the oriented DSFs gradually decreased from about 1.5 μm (Figure 4a) to 1.2–1 μm (Figure 4b) and approximately 0.6 μm (Figure 4c) as the pattern width decreased from 3 μm to 1 μm, possibly because of limited space for the self-assembly of the growing DSPs. The 2D DSPs rarely grew in the grooves and on the protuberances, which indicates that these synthesis

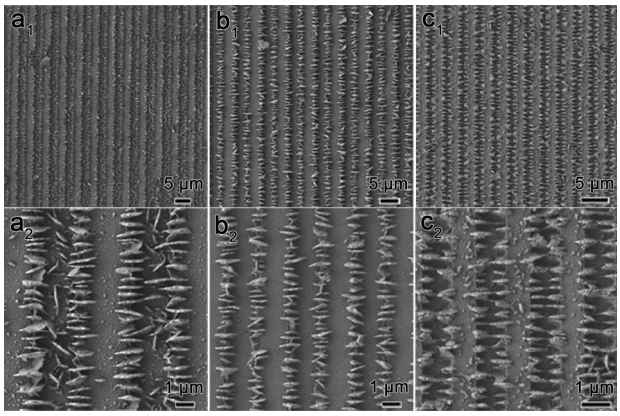

Figure 4. Arrangement of vertically aligned 2D mesostructured DSPs at the edges of a lithographically patterned substrate showing their orientation perpendicular to the longitudinal direction of the rectangular pattern. Low- and high-magnification SEM images of DSFs synthesized on surfaces with patterned widths of 3 μm (a), 2 μm (b), and 1 μm (c). The pH of the reaction solution was approximately 7.8. The molar composition of the synthesis gel was DNA/TMAPS/TEOS/H_2O/NaOH = 1:6:15:18000:1.2.

conditions allow for selectivity in both the placement and orientation of the DSPs.

The selective placement and orientation of the 2D mesostructured DSPs on the patterned substrates can be explained by the equilibrium that exists between the thermodynamic and kinetic controls for different DSP positions on the patterned silicon substrate. In this synthesis system, two competing processes, DSF growth on the supporting substrate and DSP precipitation, occur simultaneously in the synthesis gel. Both the high density of quaternary ammonium groups and the high ionization degree of DNA thermodynamically favor the formation of DSPs both on the substrate surface and in solution, whereas higher reactant concentrations and higher pH values kinetically facilitate the assembly and precipitation of DSP. A synthesis condition that allows sufficient interaction between the substrate and the reactants and simultaneously prevents DSP precipitation in the gel is needed to grow DSPs at specific positions on the substrate.

First, for the patterned substrate, the charge density of the quaternary ammonium groups on the silicon substrate surface could strongly depend on their position on the surface with the differential density of silanol groups caused by lithographic machining (with different degrees of roughness). It is possible that because of differences in the exposed surface after lithographic machining, the density of the silanol groups decreased with a decrease in surface roughness, which means that this density varied between different surface sites. Specifically, it was expected to decrease in the following order: at the edges, in the grooves, and on the protuberances (Figure S11). Correspondingly, after modification of the surface with TMAPS, the positive-charge density of the quaternary ammonium groups would have decreased in the same order at the edges, in the grooves, and on the protuberances, which results in a concomitant decrease in the thermodynamic adsorption of the DNA molecules and subsequent growth of the DSFs (Figure S11). It was difficult

to provide direct evidence of changes in the densities of the surface atoms by energy-dispersive X-ray spectrometry (EDX) in the SEM observations because the amounts of oxygen and nitrogen atoms were small compared to that of silicon. Second, in terms of the synthesis conditions, the ionization degree of negatively charged DNA molecules (phosphate groups) could be tuned by adjusting the pH of the synthesis gel because DNA is a weak polyanion with an isoelectric point of pH 4–4.5.[12] Therefore, a higher pH should render the self-assembly of DSPs more thermodynamically favorable, but the higher TMAPS concentration and pH used here favored the condensation of the silica source and led to a higher co-assembly rate (precipitation rate; Figure S11). The formation of the DSPs varied with different positions on the patterned surfaces; thus, the placement and arrangement of the DSPs on the patterned substrate surfaces were controlled by changing the pH and TMAPS concentration of the synthesis gel.

Initially, DSP formation depended on the thermodynamic effect of the highest positive charge density on the patterned substrate; thus, DSPs were formed predominantly at the edges and were always oriented perpendicularly to the longitudinal direction of the rectangular pattern under the conditions tested. Therefore, the vertically aligned DSPs were selectively placed near the edges of the patterned substrate and arranged parallel to each other in situ.

First, when DSPs formed in the grooves (Figure 2a) at lower pH and TMAPS concentration, the thermodynamic assembly and silicate condensation rates were lower (Figure S12a). Under these conditions, the growth of DSPs would be thermodynamically controlled. Therefore, DSPs grew at the edges and in the grooves where the charge density of positively charged quaternary ammonium groups was higher (Figure S11, Route A). Second, as the TMAPS concentration increased and DSPs began to grow on the protuberances (Figure 2c and 3), the DSP assembly process was gradually accelerated (Figure S12a–c). Under these conditions, the higher charge density of the quaternary ammonium groups in the grooves, which would promote the adsorption of large amounts of DNA and TMAPS and induce a higher DSP assembly rate, would lead to significant DSP precipitation, and correspondingly, the growth of DSFs would be hindered. In contrast, the DSPs that had grown near the edges extended over the entire protuberances at an appropriate pH and TMAPS concentration (Figure S11, Route B). It is possible that an intermediate TMAPS concentration resulted in DSP growth on the entire surface of the patterned substrate because of a balance between the growth of DSFs and DSP precipitation (Figure 2b). Third, for the growth of DSPs near the edges (Figure 4), increasing the pH of the reaction gel would further accelerate the assembly rate because the high ionization degree of DNA facilitates the DSP assembly with TMAPS (Figure S12c–d). Therefore, significant DSP precipitation would occur throughout the entire solution, and DSFs would only grow near the edges because the growth strongly depends on thermodynamic effects (Figure S11, Route C). At intermediate pH values, DSPs selectively grew parallel to each other near the edges and randomly oriented on the protuberances (Figure S8b).

To the best of our knowledge, this work is the first to demonstrate the selective control of the alignment, placement, and arrangement of 2D mesostructured platelets through TASA. The multilevel, hierarchical, vertically aligned 2D DSPs were selectively placed and arranged at different positions on the lithographically patterned substrate surfaces by changing the electrostatic interactions between the negatively charged DNA and the positively charged quaternary-ammonium-functionalized surface, which allowed for the thermodynamic and kinetic control of the self-assembly and epitaxial growth of DSFs in situ. The proposed approach has two important implications for oriented self-assembly. First, it offers a novel, feasible, and very promising method for the alignment, placement, and arrangement of highly charged biomolecules, such as peptides, proteins, and viruses, and their inorganic assembly with long-range order using TASA. These biomolecule–inorganic hybrid materials (especially films) might be integrated into sensitive multi-array biosensors and biodevices. Second, these materials can be used as hard templates for the synthesis of a variety of hierarchical oriented/aligned inorganic films[5b,14] that may find applications in photonics or electronics or in sensors.

Received: September 8, 2013
Published online: November 7, 2013

Keywords: DNA · hierarchical films · nanostructures · self-assembly · surface chemistry

[1] a) S. V. Patwardhan, G. Patwardhan, C. C. Perry, *J. Mater. Chem.* **2007**, *17*, 2875–2884; b) C. Sanchez, B. Julian, P. Belleville, M. Popall, *J. Mater. Chem.* **2005**, *15*, 3559–3592.

[2] a) L. Adler-Abramovich, D. Aronov, P. Beker, M. Yevnin, S. Stempler, L. Buzhansky, G. Rosenman, E. Gazit, *Nat. Nanotechnol.* **2009**, *4*, 849–854; b) S. Zhang, *Nat. Biotechnol.* **2003**, *21*, 1171–1178; c) T. Thurn-Albrecht, J. Schotter, G. Kästle, N. Emley, T. Shibauchi, L. Krusin-Elbaum, K. Guarini, C. Black, M. Tuominen, T. Russell, *Science* **2000**, *290*, 2126–2129; d) M. Sarikaya, C. Tamerler, A. K.-Y. Jen, K. Schulten, F. Baneyx, *Nat. Mater.* **2003**, *2*, 577–585; e) B. Cao, H. Xu, C. Mao, *Angew. Chem.* **2011**, *123*, 6388–6392; *Angew. Chem. Int. Ed.* **2011**, *50*, 6264–6268; f) T. Gibaud, E. Barry, M. J. Zakhary, M. Henglin, A. Ward, Y. Yang, C. Berciu, R. Oldenbourg, M. F. Hagan, D. Nicastro, *Nature* **2012**, *481*, 348–351.

[3] a) J. Y. Cheng, C. A. Ross, H. I. Smith, E. L. Thomas, *Adv. Mater.* **2006**, *18*, 2505–2521; b) P. Du, M. Li, K. Douki, X. Li, C. B. Garcia, A. Jain, D. M. Smilgies, L. J. Fetters, S. M. Gruner, U. Wiesner, *Adv. Mater.* **2004**, *16*, 953–957; c) Y. Yin, Y. Lu, B. Gates, Y. Xia, *J. Am. Chem. Soc.* **2001**, *123*, 8718–8729; d) Y. Xia, Y. Yin, Y. Lu, J. McLellan, *Adv. Funct. Mater.* **2003**, *13*, 907–918; e) M. Reches, E. Gazit, *Nat. Nanotechnol.* **2006**, *1*, 195–200.

[4] a) K. Gotrik, A. Hannon, A. Alexander-Katz, C. Ross, K. Berggren, *Science* **2012**, *336*, 1294–1298; b) J. Y. Cheng, A. M. Mayes, C. A. Ross, *Nat. Mater.* **2004**, *3*, 823–828; c) E. Kumacheva, R. K. Golding, M. Allard, E. H. Sargent, *Adv. Mater.* **2002**, *14*, 221–224; d) R. K. Joshi, J. J. Schneider, *Chem. Soc. Rev.* **2012**, *41*, 5285–5312; e) Y. Qin, R. Yang, Z. L. Wang, *J. Phys. Chem. C* **2008**, *112*, 18734–18736; f) H. Liu, X. Wu, L. Chi, D. Zhong, Q. Zhao, Y. Li, D. Yu, H. Fuchs, D. Zhu, *J. Phys. Chem. C* **2008**, *112*, 17625–17630; g) X. Wang, C. J. Summers, Z. L. Wang, *Nano Lett.* **2004**, *4*, 423–426; h) J. Kong, H. T. Soh, A. M. Cassell, C. F. Quate, H. Dai, *Nature* **1998**, *395*, 878–881.

[5] a) R. J. Kershner, L. D. Bozano, C. M. Micheel, A. M. Hung, A. R. Fornof, J. N. Cha, C. T. Rettner, M. Bersani, J. Frommer, P. W. Rothemund, *Nat. Nanotechnol.* **2009**, *4*, 557 – 561; b) A. M. Hung, C. M. Micheel, L. D. Bozano, L. W. Osterbur, G. M. Wallraff, J. N. Cha, *Nat. Nanotechnol.* **2009**, *4*, 121 – 126.

[6] B. Liu, L. Han, Y. Duan, Y. Cao, J. Feng, Y. Yao, S. Che, unpublished results.

[7] a) F. Livolant, A. Leforestier, *Prog. Polym. Sci.* **1996**, *21*, 1115 – 1164; b) Z. Reich, E. J. Wachtel, A. Minsky, *Science* **1994**, *264*, 1460 – 1463; c) F. Livolant, A. Levelut, J. Doucet, J. Benoit, *Nature* **1989**, *339*, 724 – 726; d) B. Chen, X. Zeng, U. Baumeister, G. Ungar, C. Tschierske, *Science* **2005**, *307*, 96 – 99.

[8] S. Che, Z. Liu, T. Ohsuna, K. Sakamoto, O. Terasaki, T. Tatsumi, *Nature* **2004**, *429*, 281 – 284.

[9] a) C. Jin, L. Han, S. Che, *Angew. Chem.* **2009**, *121*, 9432 – 9436; *Angew. Chem. Int. Ed.* **2009**, *48*, 9268 – 9272; b) L. Han, C. Jin, B. Liu, S. Che, *Chem. Mater.* **2012**, *24*, 504 – 511.

[10] a) Y. Wang, Y. C. Chang, *Macromolecules* **2003**, *36*, 6511 – 6518; b) J.-C. Wu, Y. Wang, C.-C. Chen, Y.-C. Chang, *Chem. Mater.* **2008**, *20*, 6148 – 6156; c) S. K. Parida, S. Dash, S. Patel, B. Mishra, *Adv. Colloid Interface Sci.* **2006**, *121*, 77 – 110.

[11] a) B. Liu, L. Han, S. Che, *Angew. Chem.* **2012**, *124*, 947 – 951; *Angew. Chem. Int. Ed.* **2012**, *51*, 923 – 927; b) B. Liu, L. Han, S. Che, *Interface Focus* **2012**, *2*, 608 – 616; c) B. Liu, L. Han, S. Che, *J. Mater. Chem. B* **2013**, *1*, 2843 – 2850.

[12] a) C. Jin, H. Qiu, L. Han, M. Shu, S. Che, *Chem. Commun.* **2009**, 3407 – 3409; b) Y. Cao, J. Xie, B. Liu, L. Han, S. Che, *Chem. Commun.* **2013**, *49*, 1097 – 1099.

[13] a) D. Pastré, O. Piétrement, S. Fusil, F. Landousy, J. Jeusset, M.-O. David, L. Hamon, E. Le Cam, A. Zozime, *Biophys. J.* **2003**, *85*, 2507 – 2518; b) J. Li, C. Bai, C. Wang, C. Zhu, Z. Lin, Q. Li, E. Cao, *Nucleic Acids Res.* **1998**, *26*, 4785 – 4786; c) Y. Song, Z. Li, Z. Liu, G. Wei, L. Wang, L. Sun, C. Guo, Y. Sun, T. Yang, *J. Phys. Chem. B* **2006**, *110*, 10792 – 10798; d) J. Lee, J. Koo, S. U. Hwang, S. Min, S. J. Ahn, Y. Roh, S. H. Park, *Curr. Appl. Phys.* **2012**, *12*, 1207 – 1211.

[14] a) H. Qi, K. E. Shopsowitz, W. Y. Hamad, M. J. MacLachlan, *J. Am. Chem. Soc.* **2011**, *133*, 3728 – 3731; b) K. E. Shopsowitz, A. Stahl, W. Y. Hamad, M. J. MacLachlan, *Angew. Chem.* **2012**, *124*, 6992 – 6996; *Angew. Chem. Int. Ed.* **2012**, *51*, 6886 – 6890; c) J. Xie, Y. Duan, S. Che, *Adv. Funct. Mater.* **2012**, *22*, 3784 – 3792.